

# **LEGIBILITY NOTICE**

**A major purpose of the Technical Information Center is to provide the broadest dissemination possible of information contained in DOE's Research and Development Reports to business, industry, the academic community, and federal, state and local governments.**

**Although a small portion of this report is not reproducible, it is being made available to expedite the availability of information on the research discussed herein.**

LA-UR--89-2808

CONFIDENTIAL

DE89 016987

Los Alamos National Laboratory is operated by the University of California for the United States Department of Energy under contract W-7405-ENG-36

TITLE: TEMPERATURE DEPENDENT EFFECTS DURING Ag DEPOSITION ON Cu(110)

AUTHOR(S): T. N. Taylor, R. E. Muenchausen, M. A. Hoffbauer, A. W. Denier van der Gon, Johannes F. van der Veen

Received by OST  
JUL 5 1989

SUBMITTED TO: The Journal of Vacuum Science and Technology, proceedings issue for the 36th National Symposium of the American Vacuum Society, October 23-27, 1989, Boston, MA

DISCLAIMER

This report was prepared as an account of work sponsored by an agency of the United States Government. Neither the United States Government nor any agency thereof, nor any of their employees, makes any warranty, express or implied, or assumes any legal liability or responsibility for the accuracy, completeness, or usefulness of any information, apparatus, product, or process disclosed, or represents that its use would not infringe privately owned rights. Reference herein to any specific commercial product, process, or service by trade name, trademark, manufacturer, or otherwise does not necessarily constitute or imply its endorsement, recommendation, or favoring by the United States Government or any agency thereof. The views and opinions of authors expressed herein do not necessarily state or reflect those of the United States Government or any agency thereof.

By acceptance of this article the publisher recognizes that the U.S. Government retains a nonexclusive, royalty-free license to publish or reproduce the published form of this contribution or to allow others to do so for U.S. Government purposes.

The Los Alamos National Laboratory requests that the publisher identify this article as work performed under the auspices of the U.S. Department of Energy.



Los Alamos Los Alamos National Laboratory  
Los Alamos, New Mexico 87545

FORM NO 838 REV  
BY NCI 2/89 5/81

DISTRIBUTION OF THIS DOCUMENT IS UNLIMITED  
MACTED

Handwritten signature

# **Temperature Dependent Effects During Ag Deposition on Cu(110)**

by

**T. N. Taylor<sup>a)</sup>, R. E. Muenchausen<sup>b)</sup>, and M. A. Hoffbauer<sup>a)</sup>  
Los Alamos National Laboratory  
Los Alamos, NM 87545**

and

**A. W. Denier van der Gon and J. F. van der Veen  
FOM Institute for Atomic and Molecular Physics  
Amsterdam, The Netherlands**

## **ABSTRACT**

The composition, structure, and morphology of ultrathin films grown by Ag deposition on Cu(110) were monitored as a function of temperature using low-energy electron diffraction (LEED), Auger electron spectroscopy (AES), and medium energy ion scattering (MEIS). Aligned backscattering measurements with 150 keV He ions indicate that the Ag resides on top of the Cu and there is no significant surface compound formation. Measurements with LEED show that the Ag is initially confined to the substrate troughs. Further deposition forces the Ag out of the troughs and results in a split  $c(2 \times 4)$  LEED pattern, which is characteristic of a distorted Ag(111) monolayer template. As verified by both AES and MEIS measurements, postmonolayer deposition of Ag on Cu(110) at 300K leads to a pronounced 3-dimensional clustering. Ion blocking analysis of the Ag clusters show that the crystallites have a (110)-like growth orientation, implying that the Ag monolayer template undergoes a rearrangement. These data are confirmed by low temperature LEED results in the absence of clusters, which indicate that Ag multilayers grow from a Ag-Cu interface where the Ag is captured in the troughs. Changes observed in the film structure and morphology are consistent with a film growth mechanism that is driven by overlayer strain response to the substrate corrugation.

## **I. INTRODUCTION**

**Overlayer film growth involving immiscible adatom and substrate combinations have generally been found to exhibit either a layer-by-layer or layer-cluster ( Stranski-Krastanov ) growth mechanism [1,2]. Because of the lattice mismatch between the two components, there is invariably a certain amount of strain produced in the initially deposited monolayers. The appearance of clustering during such film development acts as a relief mode for the interfacial strain as thick layers form to give the required bulk-like material properties, i.e. clusters have a lower free energy than the strained intermediate interface [3].**

**The growth of Ag on Cu at  $\geq 300\text{K}$  produces a sharp interface due to the immiscibility of the two materials. For this case Ag also exhibits the lower surface free energy and is the segregant surface species in a bulk mixture of the two materials. Previous studies have established that Ag deposition on the (111) [1,4] and (100) [5-7] faces of Cu proceeds by a layer-by-layer mechanism at 300K. In both cases a near-hexagonal or distorted Ag(111) monolayer template is formed. The template observed on the (100) surface with low-energy electron diffraction ( LEED ) has a  $c(10 \times 2)$  structure, which involves a few percent compression of the Ag relative to a bulk Ag(111) plane. Initial studies of the Ag/Cu(110) system at 300K have also shown a distorted Ag(111) monolayer [8,9]. However, continued deposition leads to pronounced three-dimensional (3-D) clustering. In view of the layer-by-layer behavior observed on the other two low-index faces, this layer-cluster mechanism is therefore quite unexpected. It does, however, suggest that there may be different and larger strain factors built up in the initial near-hexagonal monolayer, perhaps due to the large corrugation found on the (110) face as compared to the smoother (111) and (100) orientations. In the present study we further explore the Ag/Cu(110) growth process and describe the structure and morphology changes that are found as a function of coverage and temperature.**

## II. EXPERIMENTAL

The data were taken at two different locations on unrelated samples. One Cu(110) face was studied with medium-energy ion scattering (MEIS) measurements at the FOM-Institute in Holland while three faces on two different samples were examined with LEED and Auger electron spectroscopy (AES) at Los Alamos. The MEIS investigation involved some LEED and AES analysis. The results were consistent with the more detailed work reported at Los Alamos. Auger data reported in this paper were obtained using a LEED optics in a retarding field configuration. Similar measurements were made using a cylindrical mirror analyzer at the FOM. The MEIS study was done at 300K while the Los Alamos LEED-Augur data was taken for substrate temperatures between 120 and 350K.

Each sample was polished to a mirror finish and following either acid or electropolishing treatment was mounted on a holder and inserted into UHV. After several sputter/anneal cycles no surface impurities were detectable with AES and LEED gave a sharp integral-order spot pattern. Silver was deposited on the sample below  $2 \times 10^{-10}$  Torr at a fluence of approximately one monolayer per minute.

The MEIS measurements were performed using 150 keV He ions. Analysis of the scattered ions was facilitated using a position sensitive electrostatic detector, which measured the ion yield scattered into a slit spanning  $20^\circ$ . Combined with a very stable ion source this detector gave an experimental ion energy resolution of  $\delta E/E$  of  $3.6 \times 10^{-3}$  [10,11]. Most of the MEIS study involved scattering in a  $(1\bar{1}1)$  plane, which is oriented perpendicular to the surface and extends across the hollows formed by the row-trough configuration on the relatively open (110) face ( density =  $1.09 \times 10^{15}$  atoms  $\text{cm}^{-2}$  ). More details on the scattering geometry will be given where appropriate in the following text. The MEIS technique measures Rutherford backscattering spectra as a function of scattering angle and consequently changes in the sample crystallinity can be monitored. Shadowing effects that occur when the beam of ions is aligned with a low-index direction of the crystal generate a well defined surface peak in the

backscattering spectra. It is the analysis of the surface peak area and shape that gives an exact measure of the local substrate changes produced by the adatom-substrate interactions during the initial stages of film growth. As described previously [10], the surface peak area is a function of relaxation, reconstruction, and vibrational effects in the topmost surface atoms. The MEIS measurements in the present study of Cu(110) replicated the results of Copel et al., which show a 7.5 % inward relaxation of the topmost surface layer [12].

### **III. RESULTS**

#### **A. Auger Analysis**

As shown in Fig. 1a the deposition of Ag on Cu(110) gives strong differences in the behavior of the Ag(355eV) peak-to-peak AES intensity in  $N'(E)$  as a function of Ag coverage and sample temperature. At both temperatures the intensity exhibits a linear increase with coverage until at 300K a pronounced break is observed following deposition of a Ag(111)-like monolayer. The initial linearity is indicative of uniform growth of a monolayer thick film. In the absence of compound formation the break in slope seen in the Ag(355eV) data of Fig. 1a is due to self-shadowing of the Ag during cluster development. A comparable break is seen in the Cu(63eV) data at 300K ( see inset Fig. 1 ). As the clusters mature they begin to coalesce on the surface and eventually give a continuous Ag film. The low temperature data of Fig 1a display a smooth envelope as the Ag attains a bulk Ag Auger intensity after more than 8 ML of deposition. Both LEED and MEIS data are consistent with the assignment of the Ag(111) coverage at the breakpoint. We use the breakpoint coverage as the monolayer unit in the remainder of the paper even though, as will become apparent, the growth is much more complex than just the simple propagation of Ag hexagonal layers.

The Auger data of Fig. 1a can be understood in the framework of a simple layer-by-layer model [13]. Neglecting AES electron backscattering effects the adatom Auger intensity at the monolayer endpoints is given by

$$I_A = I_{\text{bulk}} (1 - \alpha^n) \quad \text{Eq. (1)}$$

where  $\alpha$  is the electron transmission coefficient for the adatom monolayer,  $I_{\text{bulk}}$  is the Auger intensity for a thick adatom film, and  $n$  is the number of adatom layers. The data of Fig. 1 are normalized to the bulk Ag or Cu signals and, thus,  $\alpha$  for Ag(355eV) is found to be about 0.7 for the data of Fig. 1a. Substituting this value into Eq. 1 gives the layer-by-layer endpoints ( dots ) of Fig. 1a. For the coaxially positioned sample in the LEED-Auger detection scheme of this experiment we calculate an electron escape depth of 8.9 Å, assuming a 2.35 Å interplanar spacing for Ag(111) layering. As seen by AES the growth of the Ag film at 130K is indistinguishable from a perfect layer-by-layer mechanism. It is known from UHV microscopy studies of layer-clustering systems that the number density of the clusters increases with decreasing temperature as smaller nuclei become stable on the surface [3]. Thus, in the low temperature limit the clusters become individual adatoms that are randomly scattered across the growing film. It is for a distribution such as this from a quenched layer-cluster mechanism that appears the same as a perfectly layered growth process in AES [14]. In addition, the LEED data taken on Ag/Cu(110) at the low temperatures exhibit a relatively high background, which we attribute to the disordered layering that results from a limited Ag adatom mobility.

For the simple layer-by-layer model of Eq. 1, we can write the substrate Auger intensity behavior after  $n$  layers of deposition as

$$I_S = I_{\text{Clean}} \beta^n \quad \text{Eq. (2)}$$

where  $I_{\text{Clean}}$  is the clean substrate Auger signal and  $\beta$  is the transmission coefficient through the adatom monolayer. From the inset of Fig.1a we see that  $\beta$  is approximately 0.3 for the Cu(63eV) Auger transition, which gives an electron escape

depth of 2.64 Å for this very surface sensitive Auger transition. The continued existence of the Cu(63eV) peak in the clustering region attests to the very thin monolayer film that is present between the aggregate features.

The same 300K AES data are also plotted in Fig. 1b, where the ratio of the normalized Ag(355eV) and Cu(63eV) signals is shown as a function of coverage in Ag(111) monolayers. The layer-by-layer dependence of this ratio was calculated using the above transmission coefficients and the results are shown by the dots and connecting curves in Fig 1b. Plots of layer-by-layer data will give cusps at the completion of each monolayer, with the first monolayer cusp being especially prominent as shown in Fig. 1b. The cusps result from coverage scaling of both the Cu and Ag signals. The 300K data clearly show a cusp-like feature, but due to the clustering there is a significant departure from the layer-by-layer modeling above one monolayer. For these data the cusp provides a very prominent and useful indication of the monolayer completion point.

A figure of merit for the average 3-D cluster thickness can readily be obtained using a very idealized model of the layer-cluster growth. In this instance we assume the nucleation of clusters of a fixed thickness that are restricted to grow laterally until a uniform film is obtained which has the initial cluster thickness. For the plot of Fig. 1a, this would correspond to a straight line connecting the first monolayer with the appropriate layer of uniform film thickness [8]. For the present Ag/Cu(110) data at 300K this is particularly attractive since there is a near-linear behavior of the Auger intensity as a function of coverage in the initial stages of cluster maturation. The resultant Auger signal in the clustering regime is then a coverage weighted signal resulting from the monolayer template and the clusters. The algebraic form for the adatom Auger signal for such a model is given by

$$I_A = \theta_{\text{Cluster}} \times I_{\text{bulk}} (1 - \alpha^n) + (1 - \theta_{\text{Cluster}}) \times I_{\text{bulk}} (1 - \alpha) \quad \text{Eq. (3)}$$

where  $\theta_{\text{Cluster}}$  is the fraction of the surface covered by clusters that are n layers thick.

Using the above values for  $\alpha$  and selecting clusters 8 layers thick, Eq. 3 and the comparable one for the Cu(63eV) peak give the data points shown by the "x"s in Fig. 1. The points found in Fig. 1b are significantly below the data at 300K, even though the fit to Fig. 1a is reasonably close. This is probably not due to improper choice of the cluster thickness. Rather, the discrepancy appears to be an experimental artifact arising from the acquisition of the Cu(63eV) data. It was previously found [8] that for data taken at 130K the Cu(63eV) peak systematically fell below the lowest possible value allowed by the layer-by-layer model due to the location of the peak on the steep portion of the true secondary tail in  $N'(E)$ .

## B. LEED Analysis

The LEED data taken during Ag deposition on Cu(110) at 130 and 300K show a complex variety of structural features, which give no evidence for simple registry of the Ag adatoms with the substrate. Reciprocal space features only show evidence of extended overlayer arrays. In the following we emphasize only the major aspects of this behavior. Further details of the LEED features for this system will be described in an upcoming publication [15].

Initial submonolayer coverages of Ag produce overlayer arrays that give extra diffraction features between the integral order substrate spots along the trough direction. At 300K a (5x1) pattern is found for coverages between 0.5 and 0.75 ML. For low temperature deposition a diffuse (8x1) array is seen below 0.5 ML and there is no sign of the (5x1) configuration. The observed LEED patterns are consistent with Ag confined as linear chains in the  $[1\bar{1}0]$  troughs.

Deposition approaching a monolayer coverage shows the onset of diffraction features inside the (1x1) reciprocal unit mesh that are characteristic of c(2x4) overlayer symmetry. These features are initially split in the trough direction. However, with completion of the monolayer there is an unmistakable 7th-order splitting normal to the troughs, as depicted in Fig. 2a. In addition, there are minor satellite features of higher order in the trough direction. Given that the other two low-index faces of Cu

form near-hexagonal Ag monolayers, it comes as no surprise that the basic ingredients of the split-c(2x4) pattern can be explained in a similar fashion. For the overlayer orientation of the model in Fig. 2c, where the nearest-neighbor distance of the Ag is aligned across the troughs, only a few percent distortion of a bulk Ag(111) layer is required to give a perfect c(2x4) coincidence. For such an arrangement, where there would be no splitting of the extra c(2x4) spots, there is a lattice point at the corner and center of the (2x4) mesh and each has a basis set of five Ag atoms. However, a further modification of the overlayer is needed to give the observed 7th-order splitting. This can be most simply accomplished for the planar array of Fig. 2c by compressing a bulk Ag(111) plane 2.5 % across the troughs so that the distorted c(2x4) subunit diffraction is modulated by a (2x7) overlayer mesh containing 18 Ag atoms. Clearly this model is too simple when one considers that the overlayer must be ruffled in response to the substrate corrugation. These additional factors may be partially responsible for the weak satellites seen in the monolayer spot pattern along the trough direction.

Postmonolayer deposition erases the split-c(2x4) structure. The restructuring is completed after only 2.0 ML deposition at 130K, while at 300K a completed thick film is required for final extinction of the features. This behavior agrees with the progressive roughening of the overlayer morphology that results from cluster formation as the temperature is elevated. The best measure of this structural change is found for low temperature deposition of Ag on a well ordered monolayer template formed at 300K. With the split-c(2x4) pattern completely obliterated between 2.0 and 3.0 ML, proper adjustment of the incident electron energy reveals an (8x1) multilayer array ( see Fig. 2b ). The simplest model that is consistent with these observations involves the in-trough placement of Ag as drawn in Fig. 2d. Here the Ag spacing along the troughs is close to the hard-sphere diameter for bulk Ag ( = 2.88 Å ). The initial Ag multilayers are viewed as repeating corrugated layers that preserve the symmetry of the (110) substrate. Thus, the reconstruction of the near-hexagonal monolayer involves a major relocation of the Ag. Note that the Ag separation across the troughs is the Cu trough spacing ( = 2.55 Å ), and this amounts to a 12 % reduction of the Ag spacing relative

to the trough spacing for a Ag(110) surface.

Continued deposition at the low temperature produces 3rd-order features across the troughs. At coverages from 5 - 10 ML only the multiples of the 7/8th reciprocal distance remain with their associated 3rd-order features, giving a  $(8/7 \times 3)$  diffraction pattern. Because the film is too thick at this point to allow for coincidence from the underlying substrate, the overlayer must contain some additional crystalline periodicity in the form of surface distortion or corrugation. Silver deposition to much larger coverages leads to disordering of the 3rd-order features and very diffuse LEED arrays.

### **C. MEIS Analysis**

Analysis of the overlayers formed by Ag deposition at 300K using MEIS gives information on the composition, structure, and morphology of the developing film. Most of the MEIS data were taken in an aligned condition like that shown in the Inset of Fig. 3, where the 150 keV He ion beam is incident along the  $[\bar{1}01]$  crystal direction in the  $(1\bar{1}1)$  plane. This produces distinct shadowing with a well defined Cu surface peak in the backscattering spectrum. Note that for this single alignment condition there are blocking effects that result from strings of atoms encountered as an ion scattered from below the surface exits the sample. The effect of these blocking directions is to give dips in the backscattered yield for a given component as a function of scattering angle ( angle between the incident and outgoing trajectory ). For the case shown in the inset of Fig. 3, Cu(110) has major blocking minima along the  $[011]$  and  $[121]$  strings at scattering angles of 60 and 90° , respectively.

As depicted in Fig.3, the initial stages of Ag deposition on Cu(110) at 300K lead to well resolved Ag and Cu peaks in the backscattered spectra. Importantly the Cu peak gradually decreases with coverage until stabilizing at a 30 % reduction after 0.5ML is reached for the double alignment or  $[121]$  exiting condition. This behavior rules out strong surface compound formation, where the Ag strongly reacts with and displaces the topmost Cu atoms thereby destroying the initial string perfection and increasing the Cu surface peak area. The observed reduction in Cu surface peak area can be attributed to a complex combination of direct Ag shadowing from hollow site

bonding in conjunction with substrate relaxation and vibrational effects. For the backscattering spectrum of Fig. 3 there is no contribution in the region between the Cu and Ag peaks.

Although the Ag surface peak area increased progressively with coverage the character of the backscattering spectrum remained the same as that in Fig. 3 until a coverage of 0.93 ML ( $= 1.30 \pm 0.1 \times 10^{15}$  atoms  $\text{cm}^{-2}$ ) was reached. At this point in the deposition the low energy side of the Ag peak began to expand and give a tail indicative of 3-D Ag clustering. The spectrum obtained for the highest coverage of these measurements ( $= 2.33$  ML) is shown in Fig. 4. A number of undulations are apparent in the region of the cluster contribution. These dips in the spectrum are due to blocking, which arises from the cluster crystallinity. The inset of Fig. 4 shows a cross-section obtained when the three-dimensional plot is analyzed over the cluster region of the spectrum highlighted by the shaded band. For the range of scattering angles between 80 and 100 ° there is a minimum in the yield near 92 °. Data taken for scattering angles between 50 and 70 ° at the same Ag coverage give a minimum near 63 °. Both of these values are slightly higher than the bulk blocking angles of the Cu(110) face as shown in the inset of Fig. 3. The clusters apparently are close to having a structure that is a replication of the substrate surface symmetry and bulk crystallographic orientation. This idea is quite consistent with the LEED results, where the Ag is confined in the substrate troughs at the Ag-Cu interface. This interface then serves as a (110)-like base that defines the growth direction of the Ag film.

One can estimate where such a cluster blocking minimum would occur if the Ag were allowed to propagate normal to the (110) face by replication of the substrate trough spacing. Simulations of the ion scattering from such a crystal structure were made. A continuous film model was used where hard-spheres of Ag (bulk metallic diameter) were placed in (110)-like layers with a layer unit mesh of  $3.61 \text{ \AA}$  (Cu trough spacing)  $\times 2.88 \text{ \AA}$  (Ag bulk nearest-neighbor spacing). In agreement with the simple geometric interpretation of the strings in such a distorted fcc structure, the simulations gave blocking at scattering angles much larger than those seen in Fig. 4. The elevation of the blocking angles is a consequence of placing bulk-like Ag on a shortened

rectangular unit mesh, which leads to an increase in the interplanar spacing. Blocking minima nearer to those observed in our MEIS data were obtained if the trough-like spacing were allowed to relax so that the deviation from a Ag(110) spacing was only a few percent. This notion of the cluster relaxation from the Ag-Cu interface spacing qualitatively agrees with the idea that once the film becomes three dimensional the departure from a pure fcc lattice will not be preserved due to the strain energy involved.

#### **IV. DISCUSSION**

The immiscible material behavior predicted from the binary phase properties is completely borne out during the growth of Ag thin films on Cu(110). As indicated by the AES and MEIS results there is no strong surface compound formation. Consequently the Ag-Cu interface is quite sharp and the overcoat develops independently of Ag-Cu thin film phases. The Ag overlayers never develop as an extension of simple registry relationships with the substrate, i.e. the LEED arrays are always a near-coincidence structure with many adatoms per unit mesh on top of the surface. There always appears to be an interplay between the intralayer adatom bonding and the corrugation forced on the system by the substrate.

In the initial stages of deposition linear chains of Ag are formed that are confined in the troughs. This strong modulation of the Ag structure is weakened as the troughs become filled and the Ag withdraws from the troughs to form the more Ag-like bonding configuration found in the distorted Ag(111) or c(2x4) monolayer template. Silver exhibits a lower surface free energy than Cu, and this is shown in that it is the segregant surface species in a bulk mixture of the two materials. In this context, there should be a driving force to form Ag bonds in preference to being in a Cu environment. This preference for Ag to bond to itself in the presence of Cu agrees with the observed tendency for the intralayer bonding to determine the film structure. Consequently it appears that the instability of the c(2x4) near-hexagonal template is a product of minimizing the energy in the Ag layer as opposed to a process that is dominated by

the bond energy with the Cu surface atoms. However, it should be noted that the relocation of the postmonolayer Ag into a trough-like configuration does make more intimate bonding possible to a number of Cu atoms that were totally inaccessible through the closepacked Ag monolayer. Theoretical computation of the bond and configurational energies for the various Ag/Cu(110) overlayers, which consider the Ag-Ag and Ag-Cu interactions, would be important in verifying the role played by the intralayer energy or strain in determining these structures.

Except for the small difference between the (8x1) and (5x1) chain-like overlayers seen for submonolayer coverages, the change in substrate temperature during deposition does not affect the overlayer crystallography apart from simple ordering of the arrays. However, the temperature does strongly influence the overlayer morphology during the deposition process. These effects are very pronounced for postmonolayer coverages, where at  $\geq 300\text{K}$  a pronounced layer-cluster mechanism is evident. Note that the smoother film formed in the early stages of postmonolayer growth at 130K does have the same in-trough Ag interface as that inferred for the base of the clusters from the MEIS measurements.

In line with the arguments posed above, one can rationalize the structural rearrangement from the near-hexagonal monolayer template to the (8x1) trough-like multilayers as a release of strain in the film. Apparently the c(2x4) overlayer has a high Ag surface free energy due to rumpling and perhaps defect (vacancy) content. The latter is suggested by the surface density of the c(2x4) monolayer, which is approximately 7% below that of a perfect Ag(111) bulk plane. One infers that the strain energy for the near-hexagonal Ag monolayers on the atomically smoother (111) and (100) faces of Cu is lower in view of the layer-by-layer growth found for these systems at 300K. For Ag/Cu(110) the transition to a (8x1) multilayer structure offers an alternative, but one that is far from strain free. This is evident from the heavy clustering that occurs in the absence of low temperature kinetic limitations. That is, given enough Ag adatom mobility the 3-D clusters will act as traps for the Ag. Cluster growth allows the Ag to relieve the interfacial strain and more rapidly reach a bulk-like fcc lattice.

At low temperatures the kinetics prohibit the appearance of clusters and the

strain imposed by the in-trough interface may be the reason that superlattice film periodicity ( the 3rd-order across the troughs ) is found for coverages near 10 ML. If these 3rd-order features are produced by a corrugation in the surface of the film, there is a natural comparison with the missing-row structures that have been examined by a number of researchers on (110) transition metal surfaces. Perhaps the shortening of the Ag distance across the troughs, relative to a pure Ag(110) growth, leads to a one-dimensional compression of the electron density. In effect, the strained film growth might mimic the missing-row reconstruction seen for alkali adsorption on these materials, in a process that is enhanced by the electron donation of the adsorbate [16-18]. Because clustering is not allowed at the low temperatures, it appears from the degradation of the LEED patterns at high Ag coverages that the strain is relieved in the thicker films by formation of misfit dislocations.

There are some similarities between the overlayer structures seen for Ag deposition on Cu(110) and the segregation of Au on the (110) face of a Ni - 0.8 % Au alloy [19]. The Au/Ni system not only produces the (5x1) one-dimensional array for submonolayer coverages, but it also exhibits a (2x7) phase that has the same sort of c(2x4) splitting as was seen in the present study. The latter LEED pattern was explained in terms of a compressed Ag(111) overlayer. The fact that Au is easily segregated on the alloy surface indicates that it has surface energetics that are comparable to those discussed for Ag/Cu. Apparently it is the surface bonding for these two segregation systems, coupled with the large lattice mismatch for the pairs of materials ( mismatch of 12 % for Ag/Cu and 16 % for Au/Ni ), that leads to the appearance of the near-hexagonal or segregant closepacked monolayer.

## **ACKNOWLEDGEMENTS**

The Los Alamos research was done under the auspices of the U. S. Department of Energy. The work in Holland is part of a research program of the Stichting voor Fundamenteel Onderzoek der Materie (FOM) and was made possible by the financial support from the Nederlandse Organisatie voor Wetenschappelijk. One of the authors

(TNT) would like to thank his hosts at the FOM-Institute for Atomic and Molecular Physics for their support and hospitality during his stay.

## REFERENCES

- [a] Chemical and Laser Sciences Division
- [b] Exploratory Research and Development Center
- [1] E. Bauer, *Appl. Surf. Sci.* **11/12**, 479 (1982).
- [2] J. A. Venables, G. D. T. Spiller, and M. Handbucken, *Rep. Prog. Phys.* **47**, 399 (1984).
- [3] J. A. Venables, *J. Vac. Sci. Technol.* **B4**, 870 (1986).
- [4] E. Bauer, *Surf. Sci.* **7**, 351 (1957).
- [5] P. W. Palmberg and T. N. Rhodin, *J. Chem. Phys.* **49**, 134 (1968).
- [6] J. G. Tobin, S. W. Robey, I. E. Klebanoff, and D. A. Shirley, *Phys. Rev. B* **35**, 9056 (1987).
- [7] J. E. Black, D. L. Mills, W. Daum, C. Stuhlmann, and H. Ibach, *Surf. Sci.* (in press).
- [8] T. N. Taylor, M. A. Hoffbauer, C. J. Magglore, and J. G. Beery, *J. Vac. Sci. Technol.* **A5**, 1625 (1987).
- [9] T. N. Taylor, M. A. Hoffbauer, L. Borodovsky, J. G. Beery, and C. J. Magglore, *Materials Research Society Symposia Proceedings* **83**, 95 (1987).
- [10] J. F. van der Veen, *Surf. Sci. Rep.* **5**, 199 (1985).
- [11] R. M. J. Maree, A. P. de Jongh, J. W. Derks, and J. F. van der Veen, *Nucl. Instru. and Methods in Phys. Res.* **B28**, 76 (1987).
- [12] M. W. Copel, doctoral thesis, University of Pennsylvania, 1986.
- [13] G. E. Rhead, M. - G. Barthes, and C. Argile, *Thin solid Films* **82**, 201 (1981).
- [14] J. A. Venables, J. Derrien, and A. P. Janssen, *Surf. Sci.* **95**, 411 (1980).
- [15] T. N. Taylor, R. E. Muenchausen, and M. A. Hoffbauer, in preparation.
- [16] J. W. M. Frenken, R. L. Krans, J. F. van der Veen, E. Holub-Krappe, and K. Horn, *Phys. Rev. Lett.* **59**, 2307 (1987).

- [17] P. Haberle, P. Fenter, and T. Gustafsson, Phys. Rev. B 39 , 5910 (1989).  
 [18] K. - M. Ho and K. P. Bohnen, Phys. Rev. Lett. 59 , 1833 (1987).  
 [19] E. G. McRae and R. A. Malic, Surf. Sci. 177 , 53 (1986).

## FIGURE CAPTIONS

Figure 1 - - - (a) Normalized Ag and Cu Auger peak-to-peak intensities in  $N'(E)$  for the deposition of Ag on Cu(110) at 130 and 300K.

(b) Ratio of normalized Ag and Cu Auger intensities in (a) as a function of Ag coverage for deposition at 300K.

Dots and solid lines depict a layer-by-layer behavior and "x"s are for ideal clustering model, as described in the text.

Figure 2 - - - Overlayer structures for Ag deposition on Cu(110) at one monolayer coverage and above.

Top left : split-c(2x4) LEED pattern obtained for monolayer coverage. A c(2x4) reciprocal unit mesh is indicated by the dashed lines.

Top right : (8x1) LEED pattern obtained for multilayer deposition at low temperature.

Bottom left : Real-space model of a c(2x4) overlayer based on a distorted Ag(111) array. Large circles are Ag adatoms and dots are the locations of the topmost Cu atoms. Dashed line shows the c(2x4) unit mesh.

Bottom right : Real-space model for the (8x1) layering. Circles and dots are the same as in (c).

Figure 3 - - - Backscattering spectrum showing the Ag and Cu peaks as a function of backscattering energy and scattering angle ( $\theta_S$ ) for 0.90 ML Ag deposition at 300K. Inset depicts the scattering geometry in the (1 $\bar{1}$ 1)

plane. Shadow and blocking cones are drawn for the  $[\bar{1}01]$  and  $[011]$  string directions, respectively.

**Figure 4 - - - Backscattering spectrum showing the Ag cluster contribution as a function of backscattering energy and scattering angle ( $\theta_S$ ) for 2.33 ML Ag deposition at 300K. Inset is a plot of the data for a cross-section in the shaded region of the backscattering spectrum.**

# Ag/Cu(110)

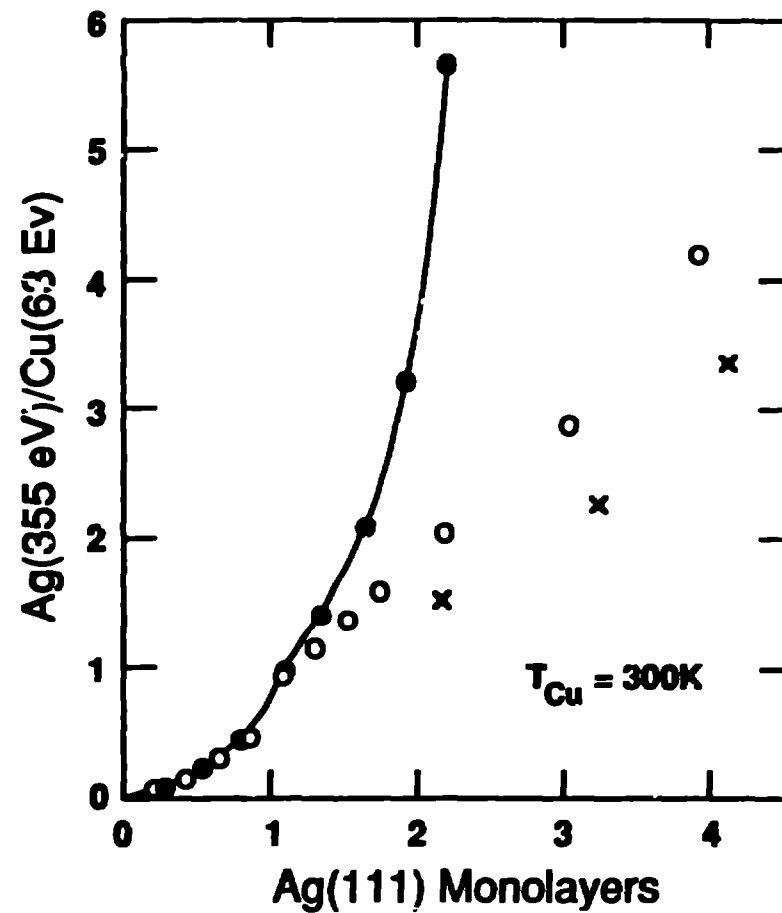
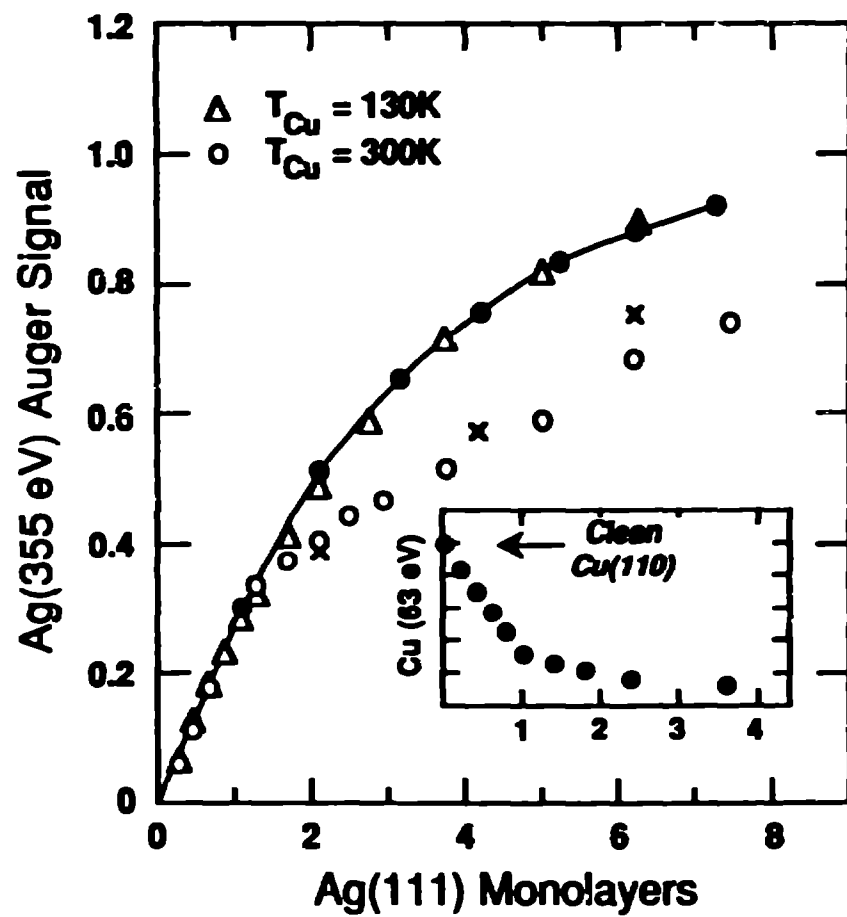
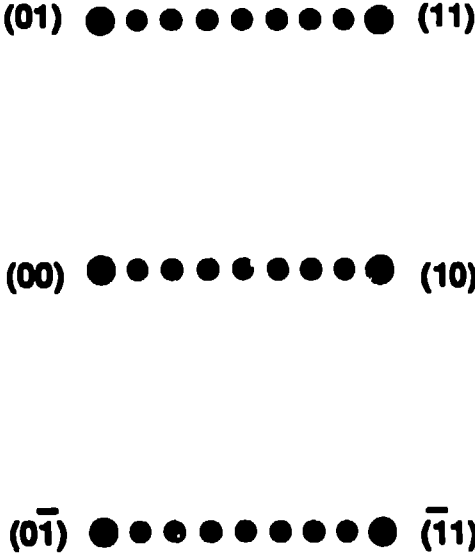
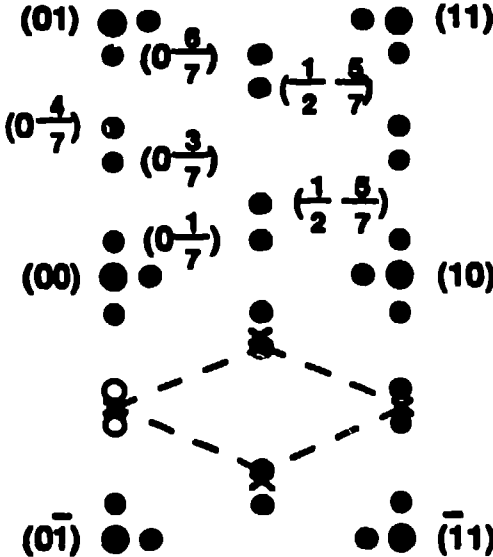
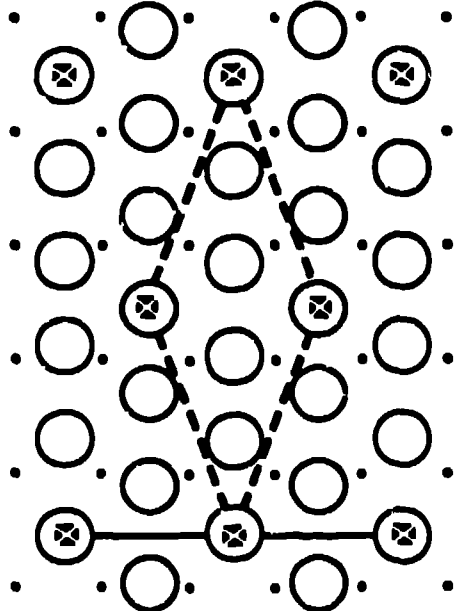


Fig. 1  
Taylor et al.

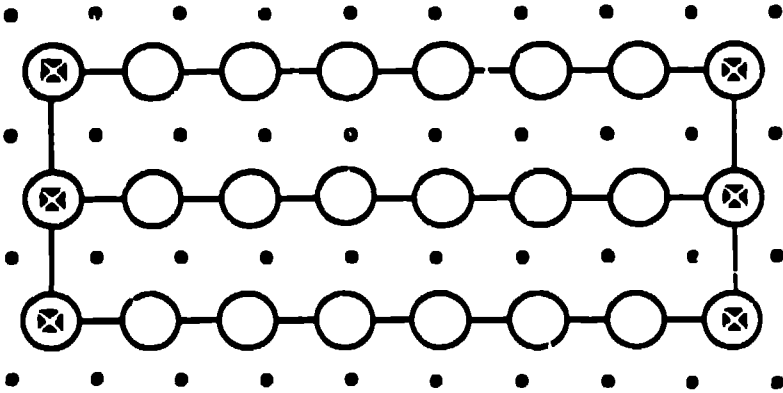
# LEED Pattern



# Model



**c(2x4)**



**(8x1)**

Fig. 2  
Taylor et al.

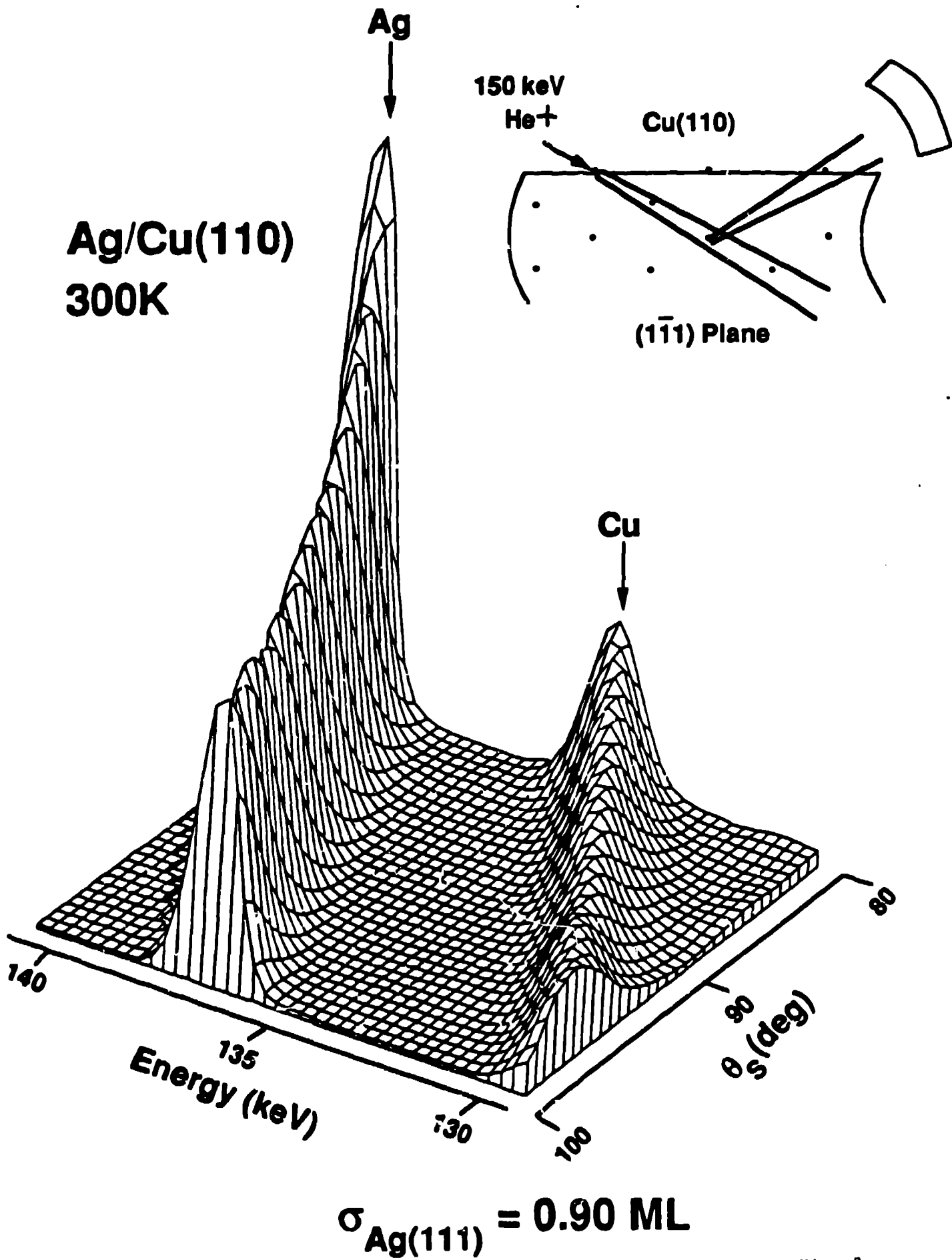
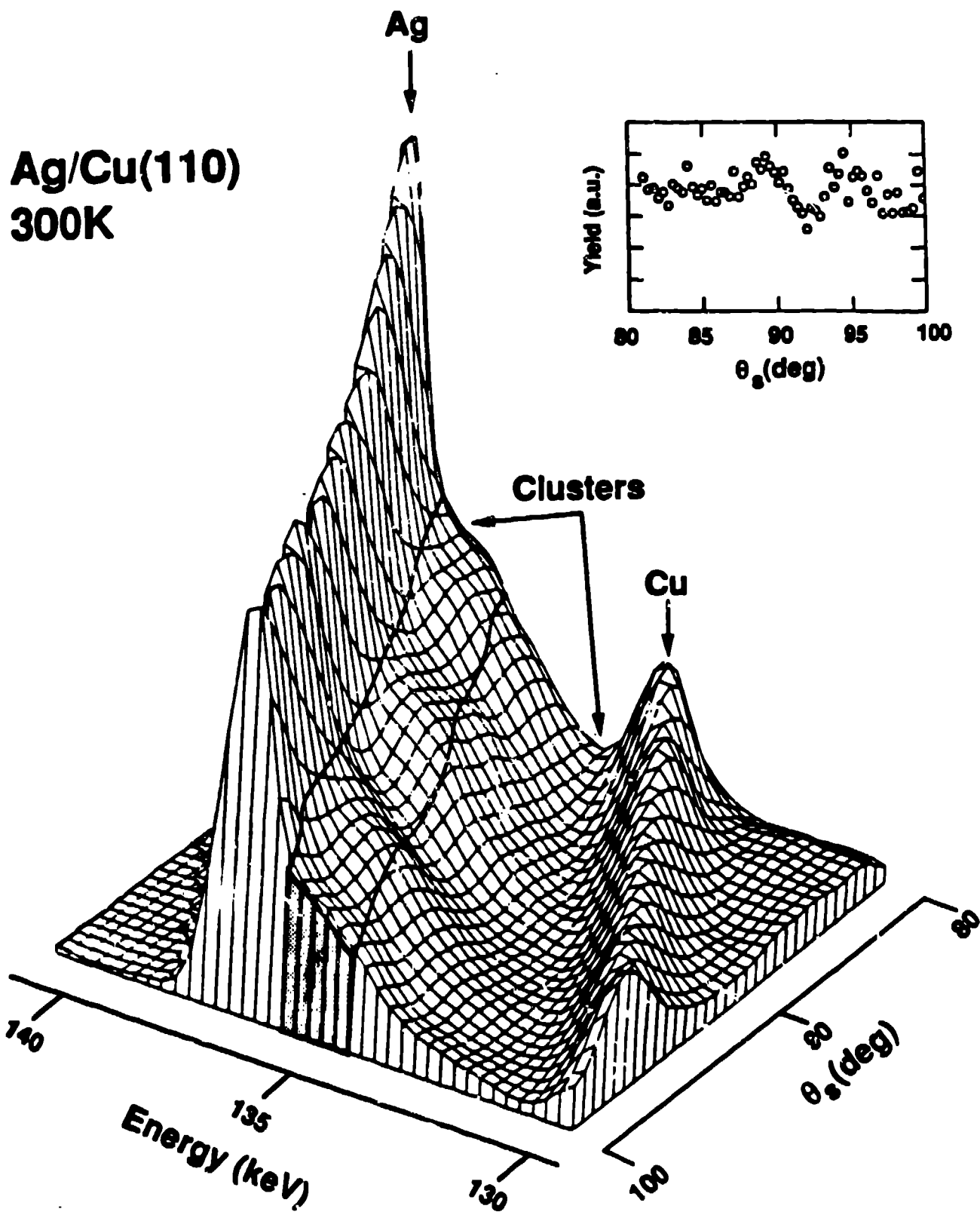


Fig. 3  
Taylor et al.



$$\sigma_{\text{Ag}(111)} = 2.33 \text{ ML}$$

Fig. 4  
Taylor et al.